



# Developing a novel neutralizing monoclonal antibody against TrkB

Gamze Eda Yildirim<sup>1</sup> · Erkan Yilmaz<sup>1</sup>

Received: 3 June 2024 / Accepted: 23 August 2024  
© King Abdulaziz City for Science and Technology 2024

## Abstract

The TrkB receptor, which is highly expressed in various human cancers and considered a pro-oncogene, was targeted to develop neutralizing monoclonal antibodies against its immunoglobulin-like (Ig-like) domains. Recombinant TrkB-IgL peptide, including the Ig-like C2 type 1 (Ig-C2-type 1) and Ig-like C2 type 2 (Ig-C2-type 2) domains, was expressed and purified from *E. coli*. Mice were immunized with this peptide, and hybridoma clones producing anti-TrkB-IgL antibodies were generated. Among 23 ELISA-positive TrkB-IgL hybridoma clones, four (TrkB-IgL 5.11, 4.11, 4.6, 4.3) showed anti-proliferative effects compared to the control on human breast cancer (MCF-7) and human colon cancer (HCT116) cells, as assessed using the xCELLigence system. Western blot analysis revealed that TrkB-IgL 5.11 and 4.11 significantly suppressed TrkB-mediated signaling pathways compared to the control. Purified TrkB-IgL monoclonal antibodies (mAbs) exhibited anti-proliferative effects compared to both positive and negative controls using the xCELLigence system. The TrkB-IgL 5.11 mAb notably suppressed phosphorylation of TrkB, Akt, and ERK and induced Caspase-3 and Caspase-9 activities in a dose-dependent manner, as determined by Western blotting. Additionally, immunostaining confirmed the localization of these mAbs on the SH-SY5Y cell membrane, which is known for high TrkB expression. In conclusion, the TrkB-IgL 5.11 antibody effectively inhibits cancer cell proliferation and induces apoptosis by suppressing key signaling pathways. These findings demonstrate the potential of this antibody as a therapeutic agent for cancers that overexpress TrkB. Additionally, it is considered a promising candidate for humanization, which would facilitate its application in cancer treatment.

**Keywords** TrkB · Neutralizing antibody · Monoclonal antibody

## Introduction

TrkB, a neurotrophin receptor and a critical member of the Trk family, exhibits high-affinity binding with brain-derived growth factor (BDNF) (Haniu et al. 1997). The TrkB/BDNF interaction plays a critical role in various biological processes associated with the maturation and development of the nervous system (Klein et al. 1989, 1993). These processes encompass neuronal differentiation, growth, invasion, and survival (Kelly-Spratt et al. 2002). Initially, research on the BDNF-TrkB signaling pathway focused on the nervous system, establishing connections to conditions such as depression, schizophrenia, and Alzheimer's disease (Numakawa et al. 2013; Hellweg et al. 2008; Shoval and Weizman 2005). However, in recent years, it has been discovered that BDNF/TrkB is highly expressed in various

cancer types and is associated with their growth, invasion, and metastasis. These include gastric cancer (Jin et al. 2021; Okugawa et al. 2013), lung cancer (Okamura et al. 2012), hepatocellular carcinoma (Guo et al. 2011; Lam et al. 2011), breast cancer (Tajbakhsh et al. 2017) as well as ovarian (Xu et al. 2019) and colon cancer (Brunetto de Farias et al. 2011; Tanaka et al. 2014; Guzel et al. 2021).

The activation of the BDNF and TrkB signaling pathway at the cellular level leads to oncogenic effects, promoting cancer cell growth, proliferation, survival, migration, and epithelial-to-mesenchymal transition. Simultaneously, it reduces anoikis, relapse, and sensitivity to chemotherapy through the RAS/MAPK, PI3K/PDK1/AKT, and PLCgamma pathways, as well as the transactivation of the epidermal growth factor receptor (Yoshii and Constantine-Paton 2010; Huang and Reichardt 2003; Thiele et al. 2009; Desmet and Peeper 2006; Nakagawara 2001; Meng et al. 2019).

In this research, the objective was to develop a neutralizing monoclonal antibody against TrkB by specifically

✉ Erkan Yilmaz  
eyilmaz@ankara.edu.tr

<sup>1</sup> Biotechnology Institute, Ankara University, Ankara, Türkiye

targeting its Ig-like domain. The antibodies, generated using a combination of recombinant biotechnology and hybridoma technology, exhibited the ability to suppress the BDNF-mediated TrkB signaling pathway and inhibit cell proliferation in MCF7 and HCT116 cells.

## Materials and methods

### The production of TrkB-IgL recombinant peptide

The human TrkB-ECD domain (corresponds to amino acids 197 to 365 and including the Ig-like C2 type 1 and Ig-like C2 type 2 domains), was targeted for production as a recombinant peptide, and the produced peptide was named TrkB-IgL.

The human neuroblastoma (NB) cell line SH-SY5Y, which expresses high levels of TrkB, was used as the source of cDNA. TrkB-IgL was amplified from the cDNA using specific primers designed with restriction endonucleases, then double digested with NdeI and BamHI, and cloned into the pET28a(+) expression vector with 6XHis tags at the C- and N-terminals. The recombinant plasmid was transformed into competent *E. coli* BL21(DE3) cells. The transformed cells were plated on LB agar containing kanamycin (50 µg/ml) and incubated overnight at 37 °C. After incubation, the selected positive clones were inoculated in LB broth containing kanamycin (50 µg/ml) and grown at 37 °C with shaking at 200 rpm until the optical density at 600 nm (OD<sub>600</sub>) reached approximately 0.5. At this point, to induce the expression of the recombinant peptide, induction medium (2% tryptone, 1 mM IPTG, 50 µg/ml kanamycin) was added to the culture. Protein expression was induced with 1 mM IPTG at 37 °C with shaking at 200 rpm for a further 4 h. Subsequently, bacterial cells containing the target gene were collected and pelleted. To lyse the cells, the pellet was resuspended in lysis buffer (0.5% Triton X-100, 0.2 µg/ml lysozyme, 50 mM Tris-HCl) and subjected to sonication for 8 min at 40% amplitude. The lysate was centrifuged, and the supernatant was collected. The obtained supernatant was loaded onto a Ni-NTA column (Thermo; Lot No: VF296224).

The recombinant protein with the His-tag was purified using Ni-NTA chromatography. Following chromatography, whole eluted proteins were analyzed by 12% SDS-PAGE and subsequently stained with Coomassie Blue. Purified fractions identified by SDS-PAGE were collected and dialyzed overnight at 4 °C against PBS to remove imidazole and other small molecules. The total protein concentration of the purified recombinant protein was determined using a BCA assay.

### The production of monoclonal antibodies by hybridoma technology

**Immunization:** the recombinant TrkB-IgL peptide (100 µg/ml) was premixed with an adjuvant and injected intraperitoneally into three 8-week-old female Balb/C mice. The mice were immunized four times at 20-day intervals. The adjuvant was emulsified with the antigen in a 1:1 ratio. For the initial immunization, complete Freund's adjuvant (CFA) was used, while incomplete Freund's adjuvant (IFA) was used for subsequent immunizations. Following four injections, blood was collected from the tail vein using a capillary. The antibody titers in the blood were assessed by ELISA with serial dilutions to evaluate the immune response. Positively tested mice were injected with a final boost of 100 µg/ml of the recombinant peptide in sterile PBS without adjuvant. All animal experiments in this study were approved by Ankara University Committees on Animal Care.

**Fusion and HAT selection:** all steps in the generation of hybridomas and monoclonal antibody production were performed using the ClonaCell™-HY Hybridoma Kit (STEMCELL Technologies; Cat: 03805). Five days after the final booster immunization, splenocytes from the sacrificed mice were collected and fused with murine myeloma cells using polyethylene glycol (PEG), according to the manufacturer's protocol.

Spleen and myeloma cells fused by PEG were incubated in ClonaCell™-HY Medium C at 37 °C with 5% CO<sub>2</sub> for 16–24 h. After incubation, the cell suspension was transferred into a semi-solid selection medium containing HAT (Hypoxanthine–Aminopterin–Thymidine; ClonaCell™-HY Medium D) and incubated at 37 °C with 5% CO<sub>2</sub> for 10–12 days. The fused cells became visible to the naked eye after incubation in the methylcellulose-based semi-solid selection medium containing HAT. From these selection media, clones were selected under the microscope in a hood and then seeded into 24-well plates containing hybridoma growth medium (ClonaCell™-HY Medium E). Supernatants from hybridoma clones grown in growth medium in 24-well plates were collected, and anti-TrkB-IgL positive clones were identified by ELISA.

**BCA assay:** the protein concentration was determined using the BCA method with the BCA Assay Kit (Takara; Cat: T9300A). The standards and working reagent were prepared based on the kit protocol and followed the steps. In brief, 200 µl of working reagent was added to each well for both standards and samples in a 96-well plate. Afterward, 25 µl of each standard and sample was added to the reagent, and then the plate was incubated at 37 °C for 30 min. Absorbance values determined at 562 nm.

**ELISA:** 96-well plates were coated with 5 µg/ml TrkB-IgL peptide in 100 µl PBS and incubated overnight at 4 °C.

After washing three times with PBS-T (0.1% Tween 20 in PBS), the plates were blocked with 5% BSA in PBS-T and incubated at room temperature for 2 h. The solution was discarded and the plates were then washed once with PBS-T. A total of 100  $\mu$ l of the primary antibody (either hybridoma supernatant or diluted immune serum at concentrations of 1:5000, 1:10,000, 1:15,000, 1:22,500, 1:50,625, 1:75,937, 1:113,906, 1:170,859, 1:256,289) was added and incubated for 2 h at room temperature. The plates were washed three times with PBS-T, then 100  $\mu$ l of mouse HRP-conjugated secondary antibody (diluted 1:5000) was added and incubated for 1 h at room temperature. After incubation, the plates were washed three times with PBS-T, and 100  $\mu$ l of TMB ELISA substrate was added to each well then incubated for 30 min at room temperature in the dark. Following incubation, 50  $\mu$ l of stop solution (2N H<sub>2</sub>SO<sub>4</sub>) was added to each well, and absorbance was measured at 450 nm.

**Cell culture:** the cell lines, MCF-7; human breast cancer, HCT116; human colon cancer, SHSY-5Y; human NB were grown in Dulbecco's modified Eagle's medium (DMEM) containing 10% FBS (fetal bovine serum), 1% pen-strep. Cells were cultured and maintained under sterile conditions at 37 °C with 5% CO<sub>2</sub> and subcultured weekly using Trypsin/EDTA.

**xCELLigence RTCA system measurements:** live cell proliferation was monitored using the xCELLigence Real Time Cell Analyzer RTCA S16 system. This label-free technology monitors cell numbers by measuring changes in impedance through gold electrodes embedded in specialized e-plates. An increase in impedance indicates that the cell proliferation rate has increased, which is reflected by a higher cell index (CI) value. The e-plate well format, with 16 wells arranged in an 8 × 2 layout from A to H, allows for duplicate testing of 8 different samples within the same experiment using the RTCA S16 system.

In this study, non-treated control cells, incubated with standard growth medium (DMEM supplemented with 10% FBS) only, were used as a negative control. Human breast cancer cell line (MCF-7) and human colon cancer cell line (HCT116) were used as target cells and treated with different hybridoma supernatants or purified mAbs, with cell impedance monitored every 15 min using the RTCA SP system.

First, 100  $\mu$ l of standard growth medium was added to each well to perform a background reading in the absence of cells. After background reading, 10,000 cells per well (MCF-7 and HCT116) were resuspended in 100  $\mu$ l of hybridoma supernatants or 10  $\mu$ g of purified mAbs and seeded into each well of the e-plate. The e-plate was incubated under the laminar flow hood for 1 h at room temperature and then placed onto the RTCA SP device located inside the incubator. The CI values were monitored every 15 min.

**SDS-PAGE and Western blot:** cells (MCF-7 and HCT116 cell lines) were treated with different concentrations of hybridoma supernatant (0.5 ml/ml, 1 ml/ml) or purified antibodies (0.5  $\mu$ g/ml, 1.5  $\mu$ g/ml) for 12 h at 37 °C with 5% CO<sub>2</sub>. After incubation, cells were washed twice with cold PBS, collected using a cell scraper, and lysed in RIPA buffer (50 mM Tris-HCl, 250 mM NaCl, 1% NP-40, 0.1% SDS) containing a protease inhibitor cocktail. Cell lysates were denatured by boiling in Laemmli buffer at 95 °C for 10 min, then loaded onto a 10–12% SDS-PAGE gel and electrophoresed. To visualize all proteins on the gel, the SDS-PAGE gel was stained with 0.1% Coomassie Blue G250 (in 10% acetic acid, 50% methanol, and 40% H<sub>2</sub>O) for 2 h at room temperature with gentle shaking. Subsequently, the gel was destained with a destaining buffer (10% acetic acid, 40% ethanol, and 50% H<sub>2</sub>O) for 30 min at room temperature with gentle shaking.

**Blotting:** proteins separated by electrophoresis were transferred to a PVDF membrane. The membrane was blocked with 5% BSA in TBS-T (Tris-buffered saline with 0.1% Tween) overnight at 4 °C, and then incubated with the primary antibody (diluted 1:1000 in 5% BSA in TBS-T) overnight at 4 °C. After washing three times with TBS-T, the membrane was incubated with HRP-conjugated secondary antibody (diluted 1:5000), followed by additional washing with TBS-T. Protein signals were detected using an ECL SuperSignal West Femto Chemiluminescent Substrate Kit (Thermo, Cat No: WK336490). The primary antibodies were used Total TrkB (Cell Signaling Lot:4603), p-TrkB (Tyr706/707; Cell Signaling Lot:4621), Total Akt (Cell Signaling Lot:9272), p-Akt (Ser473; Cell Signaling Lot:9271S), Total Erk (Cell Signaling Lot:4565), p-Erk (Thr202/Tyr204; Cell Signaling Lot:4370), Caspase 3 (Abcam ab13847), Caspase 9 (Abcam ab202068), the secondary antibody anti-mouse HRP-conjugated Antibody (Cell Signaling Lot:7076S), Beta-Tubulin (Cell Signaling Lot:2146). Beta-Tubulin was used as loading control.

**Purification of antibody:** purification of antibodies was performed according to the protocol by Jordan B. Fishman and Eric A. Berg for Protein A and Protein G antibody purification. In brief, hybridoma supernatants grown in medium containing 5% FBS were collected to a volume of approximately 1 L, diluted 1:1 with PBS buffer, centrifuged at 10,000 × g for 15 min to remove cellular debris, and then loaded onto the column. The supernatants were initially subjected to pre-purification three times using a gravity Cibacron Blue 3G-A column (CB), which is commonly used for removing albumin from the protein fraction. After pre-purification, the CB elution fractions were analyzed by SDS-PAGE to confirm that albumin was removed from the protein fraction. Flow through fractions collected from the CB column were then passed through a Protein G column at least twice using gravity. To elute the bound antibody,

0.1 M glycine (pH 2) was used, and the fractions were collected in tubes containing 2 M Tris–HCl (pH 8) to neutralize the eluted antibody. Following affinity chromatography, the purity of the eluted fractions was analyzed by 12% SDS-PAGE, and then stained with Coomassie Blue.

**Antibody isotyping:** the class, subclass, and light chain of each mAb were determined using a Rapid ELISA Mouse mAb Isotyping Kit (Invitrogen Lot: 183438005). The manufacturer's protocol was followed, which involves using pre-coated ELISA strip-well plates, specific anti-mouse heavy and light chain antibodies, TMB Substrate, and stop solution. The purified antibody was diluted to 1 µg/mL in TBS, and 50 µL of this solution was added to each well. Next, 50 µL of Goat Anti-Mouse IgG + IgA + IgM HRP Conjugate was added, mixed gently, and incubated at room temperature for 1 h. The plate was washed three times with wash buffer, and then 75 µL of TMB Substrate was added to each well. After 5–15 min, 75 µL of stop solution was added, and absorbance was measured at 450 nm. A provided template was used to determine the specific heavy and light chain identifications based on the positive responses.

**Cell viability assay:** cells (MCF-7 and HCT116 cell lines) were seeded at 10,000 cells per well and incubated for 24 h in a 96-well plate. After incubation, the purified mAbs (10 µg/ml and 20 µg/ml), Etoposide (5 µg/ml) and Cetuximab (10 µg/ml), were added to the cells and incubated at 37 °C with 5% CO<sub>2</sub> for 72 h. Subsequently, 10 µL of WST-1 solution was added directly to each well, and the plate was incubated at 37 °C for 4 h. Absorbance was then measured at 450 nm using an ELISA plate reader.

## Immunostaining

In this study, for immunofluorescence staining, coverslips were coated with poly-L-lysine, and cells were fixed according to Abcam's Immunocytochemistry and immunofluorescence protocol.

Coverslips were placed in a 24-well plate, and 200 µL of poly-L-lysine was added to each coverslip. They were then incubated in a laminar flow hood for 1 h. Subsequently, the poly-L-lysine was removed, and the coverslips were left to dry for 1 h. After drying, the coverslips were washed with DPBS (Dulbecco's phosphate-buffered saline) and allowed to dry under UV light for 30 min.

SHSY-5Y cells were transferred onto the coverslip in the plate and cultured until they reached 50–70% confluence. For cell fixation, 250 µL of 3.5% PFA was added to the cells on the coverslips in the 24-well plate, and they were incubated at room temperature for 25 min. The PFA was discarded, and the cells were washed twice with 1 ml of PBS. The round coverslips were then stored in azide-containing PBS at +4 °C. On the day of staining with the primary antibody, the coverslips were removed from +4 °C, washed three

times with PBS, and then incubated with 10 µL of primary antibody (purified mAbs) at +4 °C for 24 h. Then, the coverslips were washed three times with PBS and incubated with 10 µL of FITC-labeled secondary antibody at 37 °C for 2 h. After washing three times with PBS, they were incubated with 5 µL of 7-AAD nuclear stain for 45 min at 37 °C. Following the incubation, the coverslips were mounted on slides using a mounting medium containing Hoechst and sealed. Subsequently, images were captured using a fluorescence microscope.

**Statistical analysis:** all statistical analysis was performed with Graphpad Prism version 10.2.3 and data analyzed with ANOVA (one-way). *p* value of < 0.05 was considered statistically significant. Differences are indicated as *p* < 0.05\*, *p* < 0.01\*\*, *p* < 0.001\*\*\*.

## Results

### Production of recombinant protein TrkB-IgL and hybridoma and selection of clones

The target region (amino acid 197–365, Ig like C2 type1- Ig like C2 type2) was cloned between the NheI and BamHI restriction sites in the pET28a(+) vector, as shown in Fig. 1A. The recombinant plasmid was then transformed into *E. coli*. and protein expression was induced with IPTG. Afterward, the lysed proteins were purified using the Ni–NTA column. Subsequently, the protein products were loaded and electrophoresed using 12% SDS-PAGE and visualized with Coomassie Blue staining. The molecular weight of TrkB-IgL corresponds to a protein band with an approximate molecular weight of ~26 kDa. The SDS-PAGE results indicated in Fig. 1B that the Ni–NTA purified fractions (Lane 6 to 9) of TrkB-IgL protein were eluted with 250 mM imidazole. Lane 1: MWM; lane 2: total protein; lane 3: flow-through; lane 4: wash 1; lane 5: wash 2; lane 6: elution 1; lane 7: elution 2; lane 8: elution 3; lane 9: elution 3. The expression of TrkB-IgL peptide corresponds to a band with an approximate molecular weight of ~26 kDa. Lane 7 in Fig. 1B shows elution 2, while lanes 8 and 9 show elution 3 fractions containing the pure TrkB-IgL recombinant peptide, with a molecular weight of approximately 26 kDa and the recombinant peptide. The total protein amount of the obtained pure TrkB-IgL peptide was determined using the BCA assay.

In this study, the Ig-like domain was selected for production as a recombinant peptide. The purified recombinant peptide, obtained in its pure form, is shown in the results (Fig. 1B). The pure fractions were collected and dialyzed against PBS overnight to remove imidazole. Finally, the BCA assay was performed to determine the total protein concentration (Fig. S1).



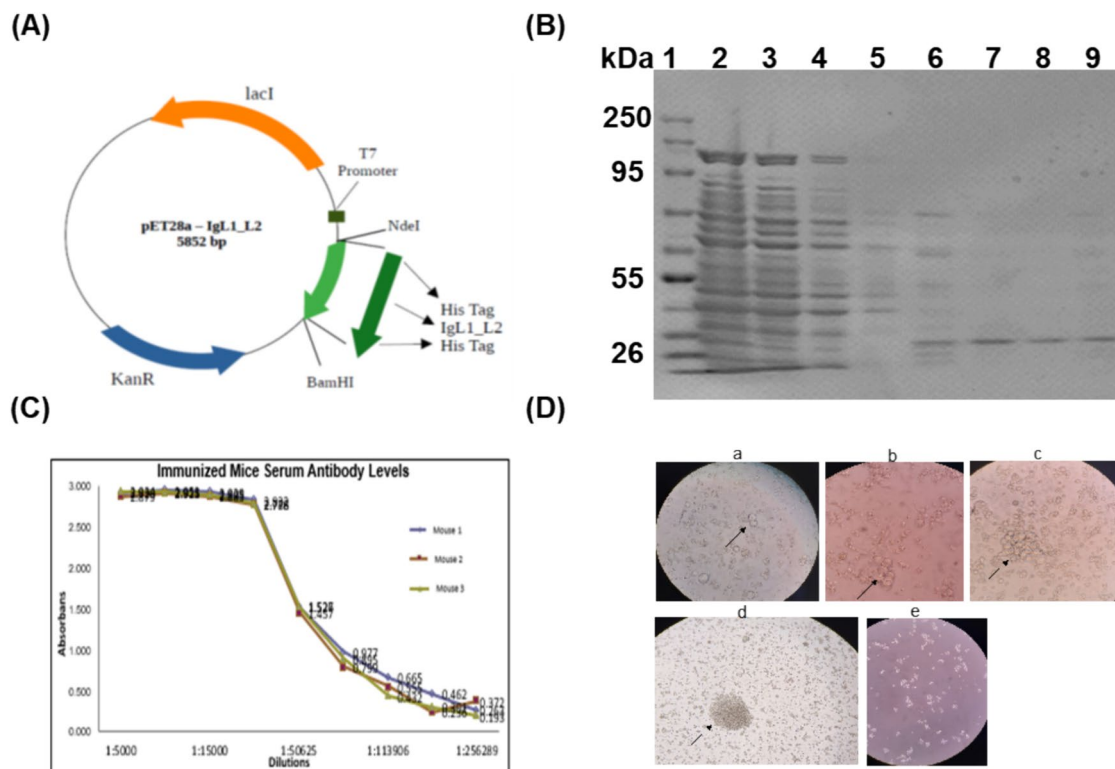


**Fig. 1** Producing recombinant peptide TrkB-IgL and anti-TrkB-IgL monoclonal antibodies (mAbs). **A** Schematic representation of the pET28(a)-TrkB-IgL vector construction. His-tag of the vector was included at N and C terminals of TrkB-IgL. The sequence of TrkB-IgL was inserted into the NdeI and BamHI restriction sites. **B** SDS-PAGE analysis of purified recombinant TrkB-IgL protein. The His-tagged proteins were purified using a Ni-NTA column after IPTG induction. The quality of the eluted pure recombinant TrkB-IgL peptide was analyzed using reduced 12% SDS-PAGE and visualized with Coomassie Blue staining. The SDS-PAGE profile shows that the Ni-NTA purified fractions (Lane 6 to 9) of TrkB-IgL protein were eluted

with 250 mM imidazole. Lane 1: MWM; lane 2: total protein; lane 3: flow-through; lane 4: wash 1; lane 5: wash 2; lane 6: elution 1; lane 7: elution 2; lane 8: elution 3; lane 9: elution 3. The expression of TrkB-IgL peptide corresponds to a band with an approximate molecular weight of ~26 kDa. **C**. Serum titration of three immunized Balb/c mice by ELISA. After the fourth immunization, blood samples were collected from the tail vein, and the titers were determined by ELISA to confirm successful immunization in all mice. **D** After fusion, the images of hybridoma clones in hybridoma growth medium under the microscope are: a) day 1, b) day 3, c) day 5, d) day 10, e) harvesting and subcloning

Blood samples were collected from the immunized mice via tail capillaries, and antibody titration in the blood was assessed by ELISA using serial dilutions. The ELISA results demonstrated that the three immunized mice generated high titers of anti-TrkB-IgL antibody (Fig. 1C). The successful immunization was proved by ELISA measurements, and the mice were boosted intraperitoneally. Following the booster injection, spleen cells from the mice were collected and fused with murine myeloma cells according to the hybridoma protocol. After fusion, hybridoma clones were cultured in the hybridoma growth medium (Fig. 1D). The supernatant of growing hybridoma cells was collected, and the antibodies against TrkB-IgL were screened by ELISA. The screening assay identified 23 hybridoma clones with the highest binding capacity, as determined by duplicate tests (Fig. S2).

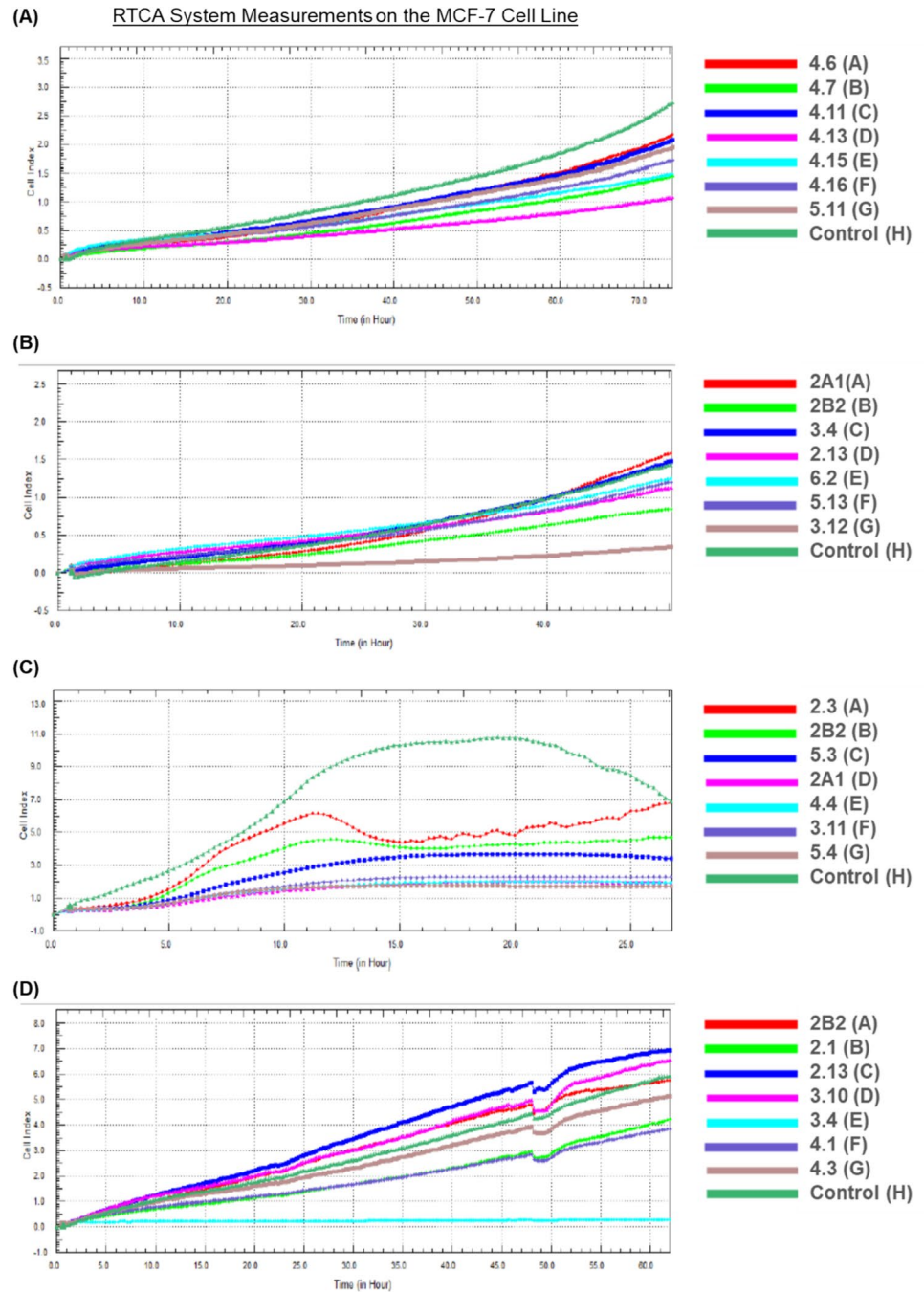
### The effect of hybridoma supernatants on cell proliferation

The effect of ELISA-positive hybridoma supernatants on the proliferation of target cells was evaluated by comparing the CI values of the control and experimental groups using the xCELLigence system.

The CI value of the non-treated control cells (green curve), incubated with standard growth medium (DMEM supplemented with 10% FBS) only, was used as a negative control for this study. The results represent the average of 2 duplicate wells.

Hybridoma supernatant was collected from 23 positive hybridoma clones and initially treated with MCF-7 cells (Fig. 2A–D). According to the CI curves of the treated cells compared to the control, 14 different hybridoma clones

**Fig. 2** Measurement of cell proliferation using the xCELLigence RTCA system. The figure illustrates the proliferation rates of cells over time as measured by the system. The results were evaluated by comparing the CI values of non-treated control cells (green curve) with those of the treated cells. **A–D** MCF-7 cells were treated with twenty-three different TrkB-IgL hybridoma supernatants, each of which was color-coded. **E, F** HCT116 cells were treated with fourteen TrkB-IgL hybridoma supernatants, which had suppressed proliferation in the MCF-7 cells. The results represent the average of 2 duplicate wells



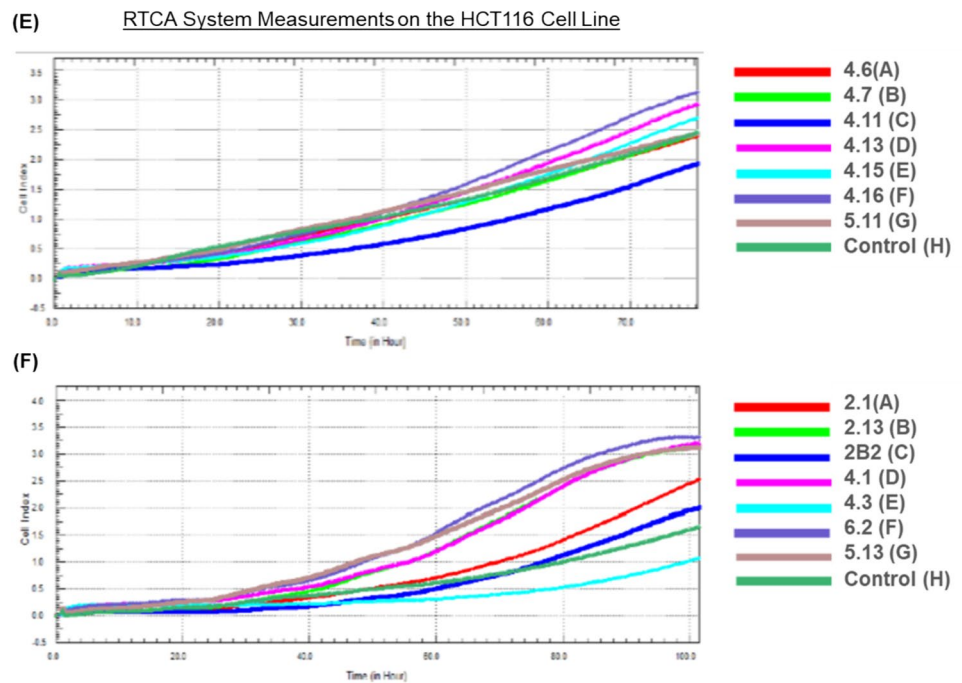
(4.6, 4.7, 4.11, 4.13, 4.15, 4.16, 5.11, 2B2, 2.13, 6.2, 5.13, 2.1, 4.1, 4.3) showed a decrease in the proliferation rate of MCF-7 cells. Subsequently, the effect of these 14 clones on cell proliferation was evaluated in HCT116 cells (Fig. 2E, F). According to the CI value results, clones 4.6, 4.11, and 5.11 in Fig. 2E, and clone 4.3 in Fig. 2F showed reduced CI values compared to the control, indicating a decrease in the proliferation rate of HCT116 cells.

xCELLigence system measurement results showed that four clones (TrkB-IgL 5.11, TrkB-IgL 4.11, TrkB-IgL 4.6,

TrkB-IgL 4.3) exhibited an anti-proliferative effect on both MCF-7 and HCT116 cancer cell lines.

Additionally, this system provides two main types of results: CI values and slope values. Slope values can be used to quantify the growth rate and assess the responsiveness of cells to treatments. The slope of the cell index curve indicates the rate at which cells are growing and dividing. A steeper slope means faster growth. Throughout the experiment, the system calculated the slope values of the cell index (Fig. 2S).

Fig. 2 (continued)



### The effect of hybridoma supernatants on the TrkB signaling pathway

Western blot analysis was performed on MCF-7 and HCT116 cell lines to assess whether TrkB-IgL 5.11, 4.11, 4.6, and 4.3 hybridoma supernatants could suppress downstream signaling pathways. The results for TrkB-IgL 5.11 and TrkB-IgL 4.11 supernatants, which showed significant results at the protein expression level, were evaluated.

The HCT116 and MCF-7 cells were treated with different concentrations of supernatants (0 ml/ml, 0.5 ml/ml, 1 ml/ml) for 12 h. They were then lysed and analyzed by Western blotting using antibodies against Akt, p-Akt, ERK1/2, p-ERK1/2, TrkB, and p-TrkB. The untreated cells were used as a control. Tubulin was used as a loading control. Western blot bands were analyzed by ImageJ and results were normalized to Tubulin.

Figure 3A shows that HCT116 cells treated with supernatant concentrations of 1 ml/ml and 0.5 ml/ml exhibited significant suppression in the p-AKT/AKT ratio for both TrkB-IgL 5.11 and TrkB-IgL 4.11, while the p-ERK/ERK ratio was suppressed only at a concentration of 0.5 ml/ml for these supernatants compared to the untreated control group. Both supernatant concentrations (1 ml/ml and 0.5 ml/ml) showed significant suppression compared to the control.

Figure 3B shows that MCF-7 cells treated with supernatant concentrations of 1 ml/ml and 0.5 ml/ml exhibited significant suppression of the p-AKT/AKT ratio for TrkB-IgL 5.11. TrkB 4.11 also suppressed the p-AKT/AKT ratio at both concentrations. TrkB-IgL 5.11 at a concentration of 0.5 ml/ml exhibited significant suppression in the p-ERK/

ERK ratio, while TrkB-IgL 4.11 decreased the phosphorylation of the p-ERK/ERK ratio at both concentrations compared to the control.

Figure 3C shows the expression levels of p-TrkB and TrkB proteins. In the left panel, TrkB 5.11 and TrkB 4.11 showed suppression of the p-TrkB/TrkB ratio at both concentrations in HCT116 cells compared to the control. In the right panel, only TrkB-IgL 5.11 supernatant at a concentration of 1 ml/ml showed suppression of the p-TrkB/TrkB ratio in MCF-7 cells compared to the control. Statistical analyses were performed using one-way ANOVA ( $p < 0.05^*$ ,  $p < 0.01^{**}$ ,  $p < 0.001^{***}$ ). Each bar represents mean  $\pm$  standard deviation of three independent experiments.

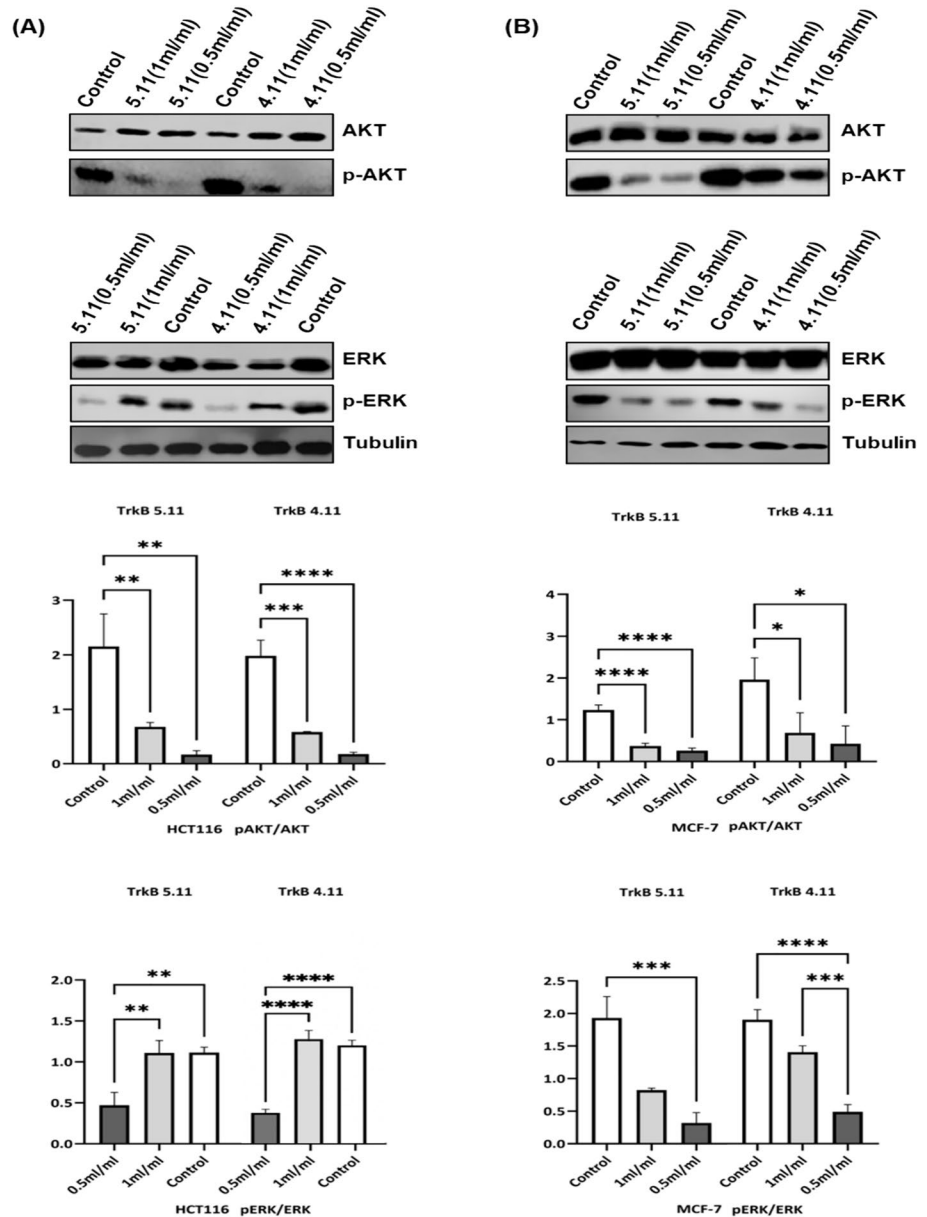
### Antibody purification by protein G

The TrkB-IgL 5.11 hybridoma supernatant, from the hybridoma culture grown with 5% FBS, was initially subjected to pre-purification three times using a CB column.

The elution fractions collected from the CB column were analyzed by SDS-PAGE and visualized with Coomassie Blue staining. The results from the reduced SDS-PAGE for the second CB column, shown in Fig. 4A lanes 3 and 4, indicate that the CB elution fractions display a distinct band at the 60 kDa molecular weight position, corresponding to albumin. This band proves that the albumin was significantly retained by the CB column.

After pre-purification, the flow-through fractions collected from the CB column were then passed through a Protein G column, and the elutions were analyzed using a reduced SDS-PAGE. The gel was stained with Coomassie

**Fig. 3** Analysis of the effect of hybridoma supernatants on the TrkB signaling pathway using Western blot (WB). The MCF-7 and HCT116 cells were treated for 12 h with 1 ml/ml and 0.5 ml/ml hybridoma supernatant. Extracts were analyzed for pAkt-to-Akt, pERK1/2-to-ERK1/2, and pTrkB-to-TrkB ratios in HCT116 and MCF-7 cells. Protein expression of Akt, pAkt, ERK1/2, and pERK: top row shows WB bands, graphs show quantitative analysis. **A** HCT116 cells; **B** MCF-7 cells. Shows TrkB and p-TrkB expression: **C** in HCT116 cells; **D** in MCF-7 cells. The untreated cells were used as a control. Statistical analyses were performed using one-way ANOVA ( $p < 0.05^*$ ,  $p < 0.01^{**}$ ,  $p < 0.001^{***}$ ). Each bar represents mean  $\pm$  standard deviation of three independent experiments, with values normalized to the Tubulin



Blue to visualize the heavy and light chain bands. The initial Protein G column purification, as shown in Fig. 4A, lane 5 (elution 1) and lane 6 (elution 3), indicates a distinct band at the 50 kDa molecular weight position corresponding to the antibody heavy chain and a band at the 25 kDa molecular weight position corresponding to the IgG light chain.

To obtain a highly pure and acceptable product from the elutions, all Protein G eluates were pooled and reprocessed through the Protein G column. The elutions were collected and analyzed by SDS-PAGE. The results of the final purification using the Protein G column, as shown in Fig. 4B lane 3 (elution 1) and lane 4 (elution 2), indicated that the heavy and light chains of TrkB-IgL 5.11 were detected as a highly pure product, and the albumin was completely removed.

In Fig. 4B, lanes 5 and 6 visualized the final CB column eluates.

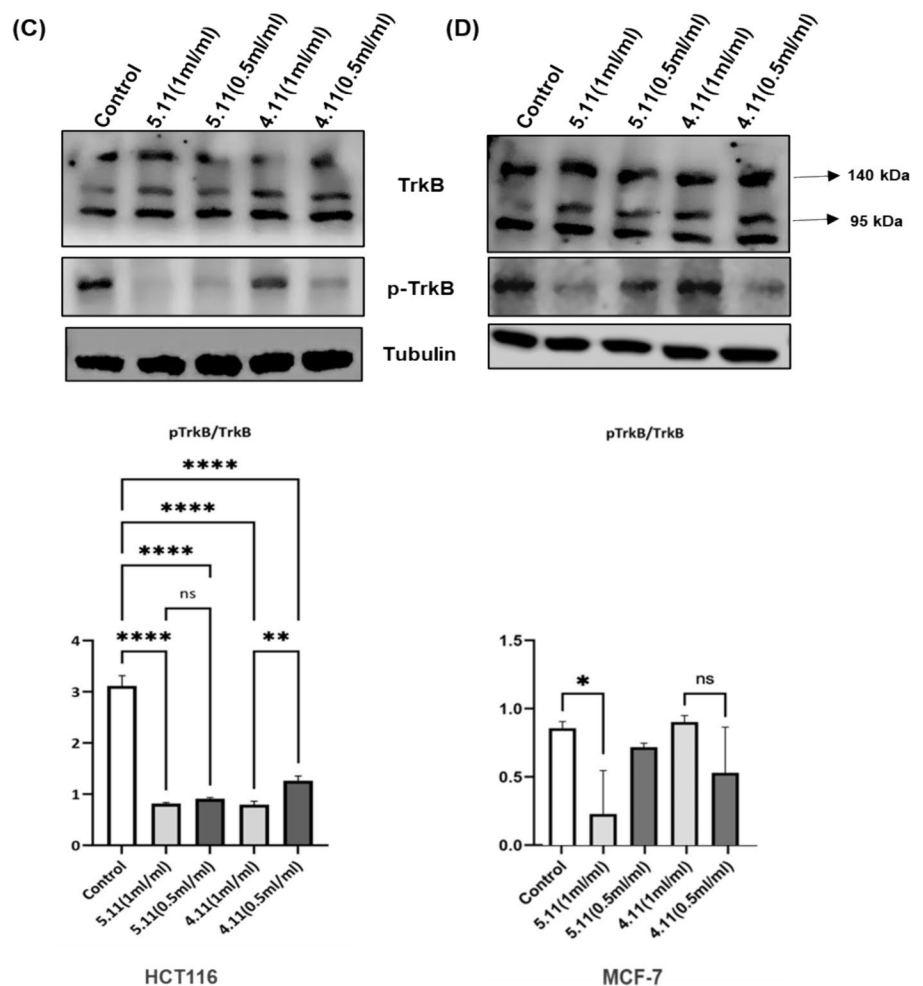
### Effects of purified mAbs on cell proliferation and cell viability assay

The cytotoxicity of the purified mAbs (10  $\mu$ g/ml and 20  $\mu$ g/ml) in HCT116 and MCF-7 cells was evaluated using WST-1. Untreated cells were used as a control. The absorbance value of the control cells was assumed to represent 100% viability for normalization, and the average of five separate measurements was used for all samples.

The results indicated that in Fig. 4C, D, the presence of TrkB-IgL 4.3 at a 10  $\mu$ g/ml concentration and Etoposide at 5  $\mu$ g/ml decreased cell viability compared to the control



Fig. 3 (continued)



group, while TrkB 5.11, 4.11, 4.6, and Cetuximab at a 10  $\mu\text{g}/\text{ml}$  concentration did not change cell viability in both cell lines.

Figure 4S shows that the presence of TrkB-IgL 4.3 and TrkB-IgL 4.11 at a 20  $\mu\text{g}/\text{ml}$  concentration, as well as Etoposide at a 10  $\mu\text{g}/\text{ml}$  concentration, significantly decreased cell viability compared to the control group in HCT116 cells. At a 20  $\mu\text{g}/\text{ml}$  concentration, TrkB-IgL 4.3 and the positive control Etoposide significantly decreased cell viability compared to the control group in MCF-7 cells.

The effect of four different purified TrkB-IgL antibodies (TrkB-IgL 5.11, TrkB-IgL 4.11, TrkB-IgL 4.6, TrkB-IgL 4.3) on cell proliferation was evaluated using xCELLigence, as described above. In this experiment, Etoposide (5  $\mu\text{g}/\text{ml}$ ) and Cetuximab (10  $\mu\text{g}/\text{ml}$ ), known to have a suppressive effect on tumor cell proliferation, were used as positive controls. The group containing only target cells and growth medium was used as the negative control.

According to the CI curves obtained from real-time cell analysis, the results showed that in Fig. 4E for MCF-7 cells and Fig. 4F for HCT116 cells, the CI value increased in the negative control group, while it was suppressed in the

positive control and experimental groups. This data revealed that all purified TrkB-IgL mAbs exhibited an anti-proliferative effect on both the MCF-7 and HCT116 cell lines.

### Antibody isotyping

The isotypes of each antibody were determined using the Rapid ELISA Mouse mAb Isotyping kit, and the concentrations of the purified antibodies were measured using the BCA Assay (Table 1).

### The effect of purified mAbs on the TrkB signaling pathway

The effect of 4 different purified TrkB-IgL mAbs (TrkB-IgL 5.11, TrkB-IgL 4.11, TrkB-IgL 4.6, TrkB-IgL 4.3) on the suppression of downstream TrkB signaling pathways was assessed using Western blot analysis. However, only the TrkB-IgL 5.11 antibody showed statistically significant suppression, so only this antibody was considered in the results. MCF-7 and HCT116 cells were treated with purified TrkB-IgL 5.11 mAb at various concentrations (0  $\mu\text{g}/$

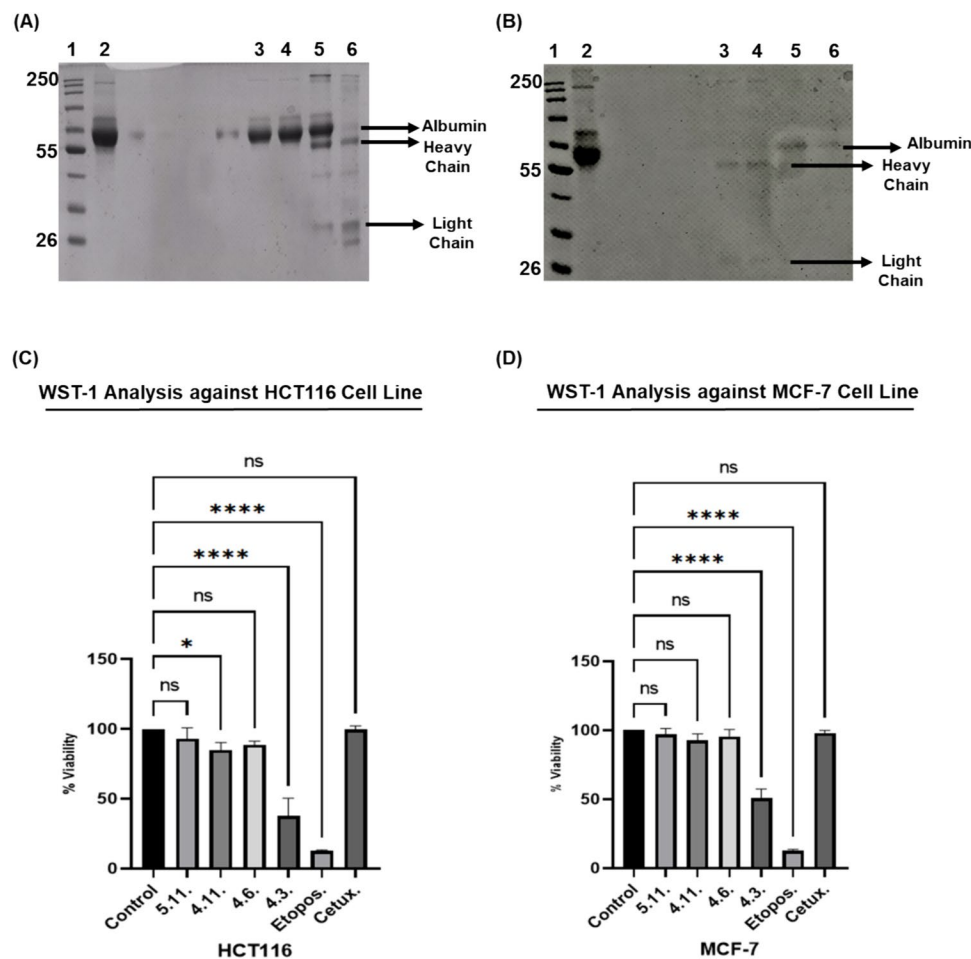


**Fig. 4** SDS-PAGE Analysis of Antibody Purification Steps and the Effects of Purified mAbs on Cell Viability and Proliferation. **A, B** SDS-PAGE analysis of purified TrkB-IgL 5.11 mAb was performed using Cibacron Blue (CB) and Protein G columns. Samples were loaded on a 12% gel under reducing conditions and stained with Coomassie Blue. **A** Eluates from the CB column (second time) and Protein G column (first time) from the TrkB-IgL 5.11 clone: lane 1, MWM; lane 2, hybridoma supernatant; lane 3, CB elution 2; lane 4, CB elution 3; lane 5, Protein G elution 1; lane 6, Protein G elution 3. **B** Pooled Protein G elutions reprocessed through the Protein G column: lane 1, MWM; lane 2, hybridoma supernatant; lane 3, Protein G Elution 1; lane 4, Protein G Elution 2; lanes 5 and 6, CB column

elution 3. **C, D** Analysis of cell viability using the WST-1 assay after a 24-h treatment with purified mAbs at a concentration of 10  $\mu\text{g/ml}$ , and Cetuximab and Etoposide at 5  $\mu\text{g/ml}$ , in **C** HCT116 cells and **D** MCF-7 cells. Statistical analyses were performed using one-way ANOVA  $p < 0.05$ ;  $n = 5$ . **E, F**. Measurement of purified TrkB-IgL mAbs on cell proliferation using the xCELLigence RTCA system. The results were evaluated by comparing the Cell Index (CI) values of non-treated control cells (green curve) with those of the treated cells. **E** MCF-7 cells and **F** HCT116 cells were treated with purified mAbs at a concentration of 10  $\mu\text{g/ml}$ , and Cetuximab and Etoposide at 5  $\mu\text{g/ml}$

ml, 0.5  $\mu\text{g/ml}$ , 1.5  $\mu\text{g/ml}$ ) for 12 h. Subsequently, the same steps as in the previous Western blot were followed, and the expression levels of the same proteins were assessed.

The phosphorylation levels of downstream signaling proteins AKT, ERK1/2 and TrkB represented by the accumulation of p-AKT/AKT, p-ERK/ERK and p-TrkB/TrkB ratios, showed the following pattern:

Western blotting results indicated that Fig. 5A HCT116 cells treated with 1.5  $\mu\text{g/ml}$  and Fig. 5B MCF-7 cells treated with 1.5  $\mu\text{g/ml}$  exhibited significant suppression in both the p-AKT/AKT and p-ERK/ERK ratios compared to the untreated control group. The pTrkB/TrkB ratio decreased

at a concentration of 1.5  $\mu\text{g/ml}$  in both HCT116 (C) and MCF-7 (D) treated samples.

### Caspase activity

Previous studies have shown that MCF-7 cells have a deficiency in caspase-3 due to a partial deletion in the caspase-3 gene (Lopez-Suarez et al. 2016).

In this study, dose-dependent activities of Caspase 3 and Caspase 9 in response to TrkB-IgL mAbs were evaluated in HCT116 cells using Western blotting. Etoposide and Cetuximab, which are known to show caspase activity, were used

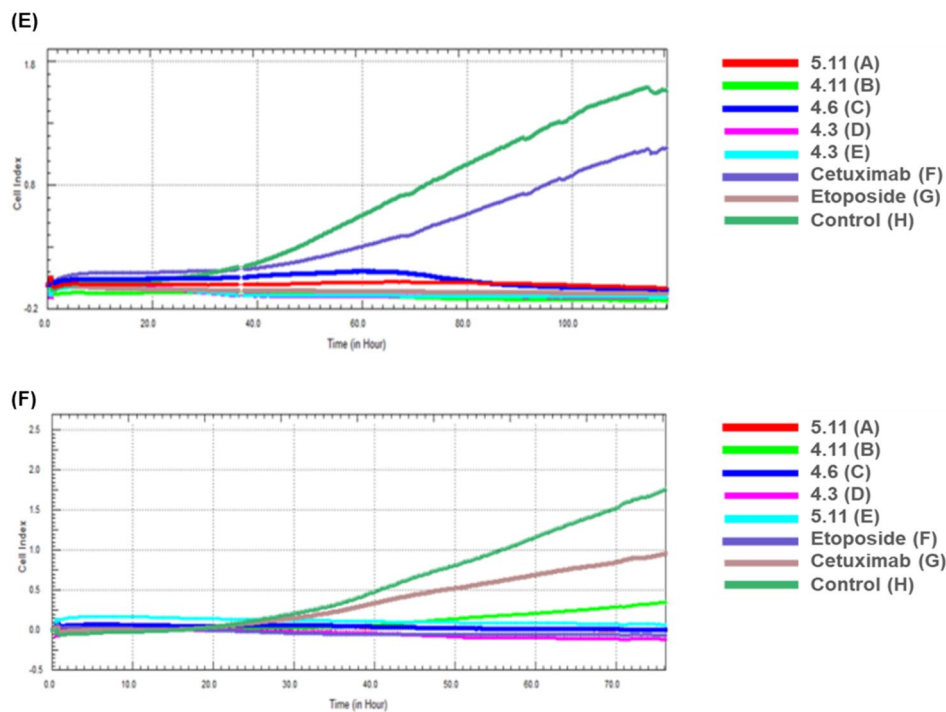


Fig. 4 (continued)

as positive controls. The untreated cells were used as a control. Western blot bands were analyzed by ImageJ, and active caspase results were normalized to Tubulin.

Western blot results showed that, as shown in Fig. 6, only the TrkB 5.11 antibody specifically demonstrated caspase 3 activity in Fig. 6A and caspase 9 activity in Fig. 6B at a concentration of 1.5  $\mu\text{g}/\text{ml}$ , compared to the control. As expected, for both caspase 3 and caspase 9, almost no activity was observed in the control group, while significant activity was observed in both positive controls.

### Immunofluorescence staining

Immunofluorescence staining was performed to demonstrate the distribution and localization of TrkB-IgL antibodies binding to the TrkB receptor on SH-SY5Y cells. This technique was used to determine the localization of

the developed pure anti-TrkB IgL mAbs on the SH-SY5Y cell membrane. SH-SY5Y cells were grown on coverslips and then stained with four anti-TrkB IgL mAbs (primer Ab) and an anti-mouse FITC secondary antibody (green). Nuclei were stained with 7-AAD (red). The localization of anti-TrkB IgL mAbs was compared with a control sample that did not contain the primary antibody (TrkB-IgL).

In Fig. 7, the staining results observed under the microscope showed that the green fluorescence significantly indicated the cellular localization of each TrkB-IgL antibody on the membrane compared to the control group. No proteins were detected by immunofluorescence in the control group, which was labeled with only the secondary antibody and did not contain the primary antibody.

### Discussion

TrkB, a receptor known for its neuroprotective and neurotrophic effects in the central nervous system, has been a focal point in studies developing agonist antibodies. These effects are linked to the receptor's expression and activation, which demonstrate potential therapeutic effects (Wu et al. 2019; Qian et al. 2006). However, TrkB is also highly expressed in various cancer types, where it plays an oncogenic role. This study aimed to produce TrkB-IgL antagonist antibodies targeting the Ig-like domains located in the extracellular

**Table 1** Isotypes of Monoclonal Antibody and Concentration Analysis by ELISA and BCA

mAb	Murine IgG isotype	Ig concentration ( $\mu\text{g}/\text{ml}$ )
TrkB-IgL 5.11	IgM, k	64
TrkB-IgL 4.11	IgG1, k	76
TrkB-IgL 4.6	IgG1, k	80
TrkB-IgL 4.3	IgG1, k	100

**Fig. 5** Analysis of the effect of purified TrkB-IgL 5.11 antibody on the TrkB signaling pathway using WB. MCF-7 and HCT116 cells were treated with various concentrations of purified TrkB-IgL 5.11 mAb for 12 h. Extracts were analyzed for pAkt-to-Akt, pERK1/2-to-ERK1/2, and pTrkB-to-TrkB ratios. Protein expression of Akt, pAkt, ERK1/2, and pERK: top row shows WB bands, graphs show quantitative analysis. **A** HCT116 cells; **B** MCF-7 cells. Shows TrkB and p-TrkB expression: **C** in HCT116 cells; **D** in MCF-7 cells. The untreated cells were used as a control. Statistical analyses were performed using one-way ANOVA ( $p < 0.05^*$ ,  $p < 0.01^{**}$ ,  $p < 0.001^{***}$ ). Each bar represents mean  $\pm$  standard deviation of three independent experiments, with values normalized to the Tubulin

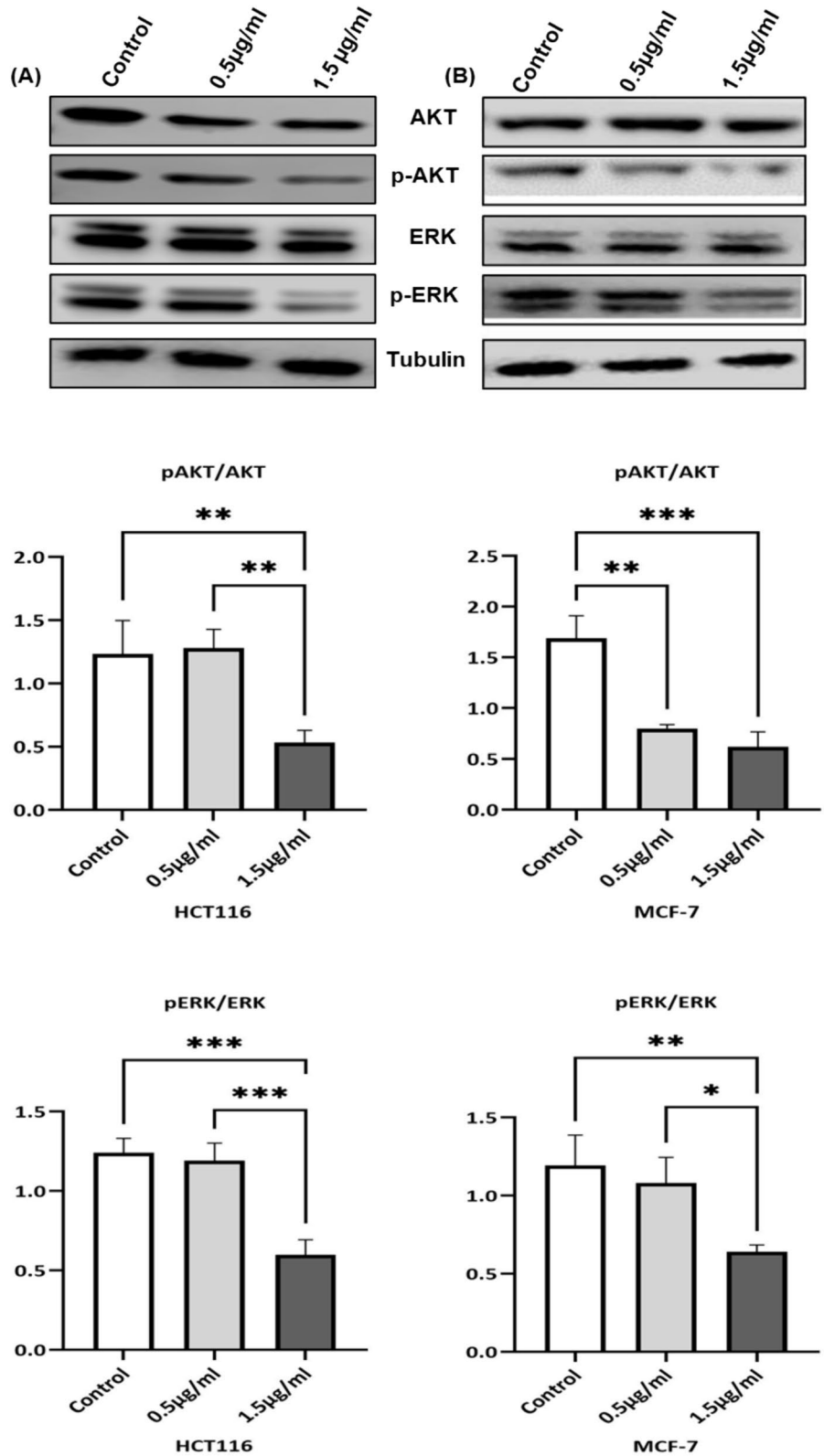
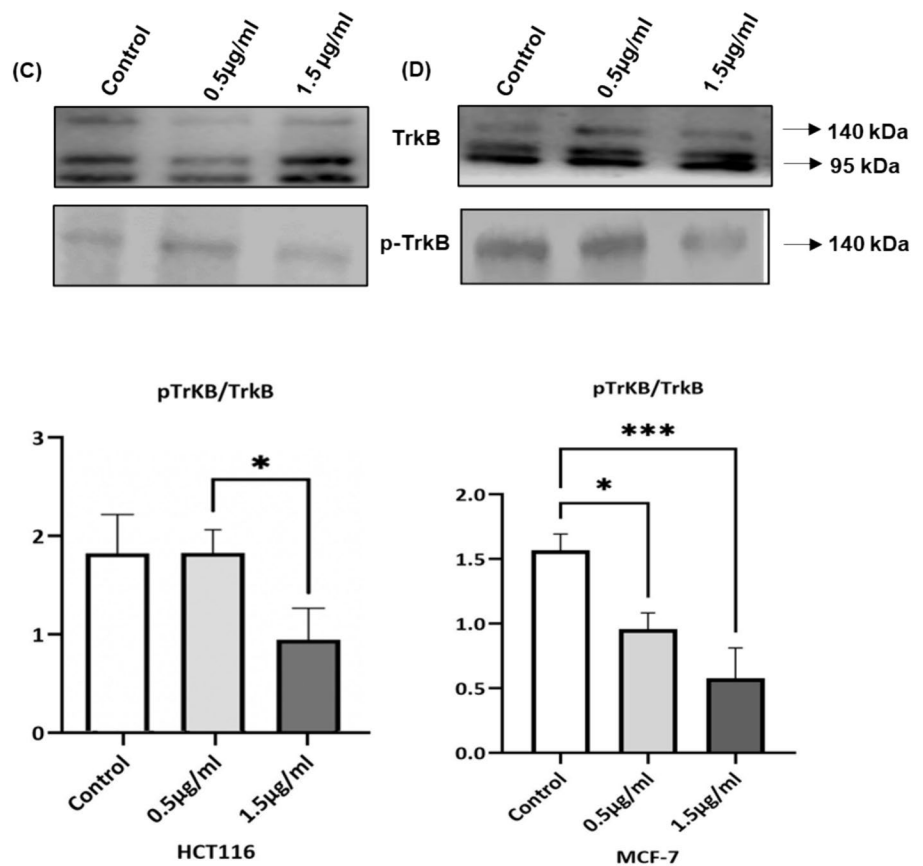




Fig. 5 (continued)



region of the human TrkB receptor using recombinant biotechnology and hybridoma technology.

BDNF, a specific ligand for TrkB, interacts with the receptor through its Ig like-C2 type 1 and Ig like-C2- type 2 domains. The type 1 subdomain, located near the surface, regulates ligand-independent activation, while the type 2 subdomain controls specific ligand binding and TrkB activation (Zaccaro et al. 2001; Arevalo and Wu 2006; Middlemas et al. 1991). Based on this, the Ig-like domains was targeted and amplified using specific primers. It was obtained in its pure form as a recombinant peptide, as showed in the result (Fig. 1B). Monoclonal antibodies against TrkB-IgL were produced using the hybridoma method, resulting in 23 different antibodies that were determined to bind to TrkB with high affinity, as determined by ELISA. The effects of these antibody supernatants on cancer cell proliferation were assessed using a real-time cell analysis system with human breast cancer and colon cancer cells.

Cell proliferation analyses revealed that antibody supernatants TrkB-IgL 5.11, 4.11, 4.6, and 4.3 exhibited anti-proliferative effects, significantly reducing the proliferation rate compared to the control in MCF-7 and HCT116 cells (Fig. 2). Western blot analysis further showed that the TrkB-IgL 5.11 and 4.11 clones suppressed the p-AKT/AKT and p-ERK/ERK ratios, which are key signaling pathways

involved in cancer cell survival and proliferation (Fig. 3A, B).

The expression levels of p-TrkB and TrkB proteins showed suppression in HCT116 cells with both TrkB-IgL 5.11 and TrkB-IgL 4.11 compared to the control, while in MCF-7 cells, only TrkB-IgL 5.11 exhibited suppression compared to the control (Fig. 3C, D).

TrkB-IgL 5.11, 4.11, 4.6, and 4.3 hybridoma clones were purified using a Protein G column. The highly purified TrkB-IgL 5.11 antibody was then analyzed using SDS-PAGE, as shown in Fig. 4B. All purified TrkB-IgL mAbs were further assessed for their effects on cell viability and intracellular signaling. Etoposide and Cetuximab were used as positive controls to evaluate the efficacy of the purified antibodies.

During the assessment of cell proliferation and viability in target cancer cells using purified mAbs, Etoposide and Cetuximab were used as positive controls.

Etoposide, one of the most commonly used chemotherapy agents, initially inhibits the cell cycle in target cancer cells, followed by the activation of apoptotic pathways (Day et al. 2009; Goloudina et al. 2012). Cetuximab is a chimeric monoclonal antibody that targets the human epidermal growth factor receptor (EGFR). Previous studies have shown that Cetuximab inhibits the growth of HCT116 cells in a dose-dependent manner. It binds to EGFR, preventing receptor

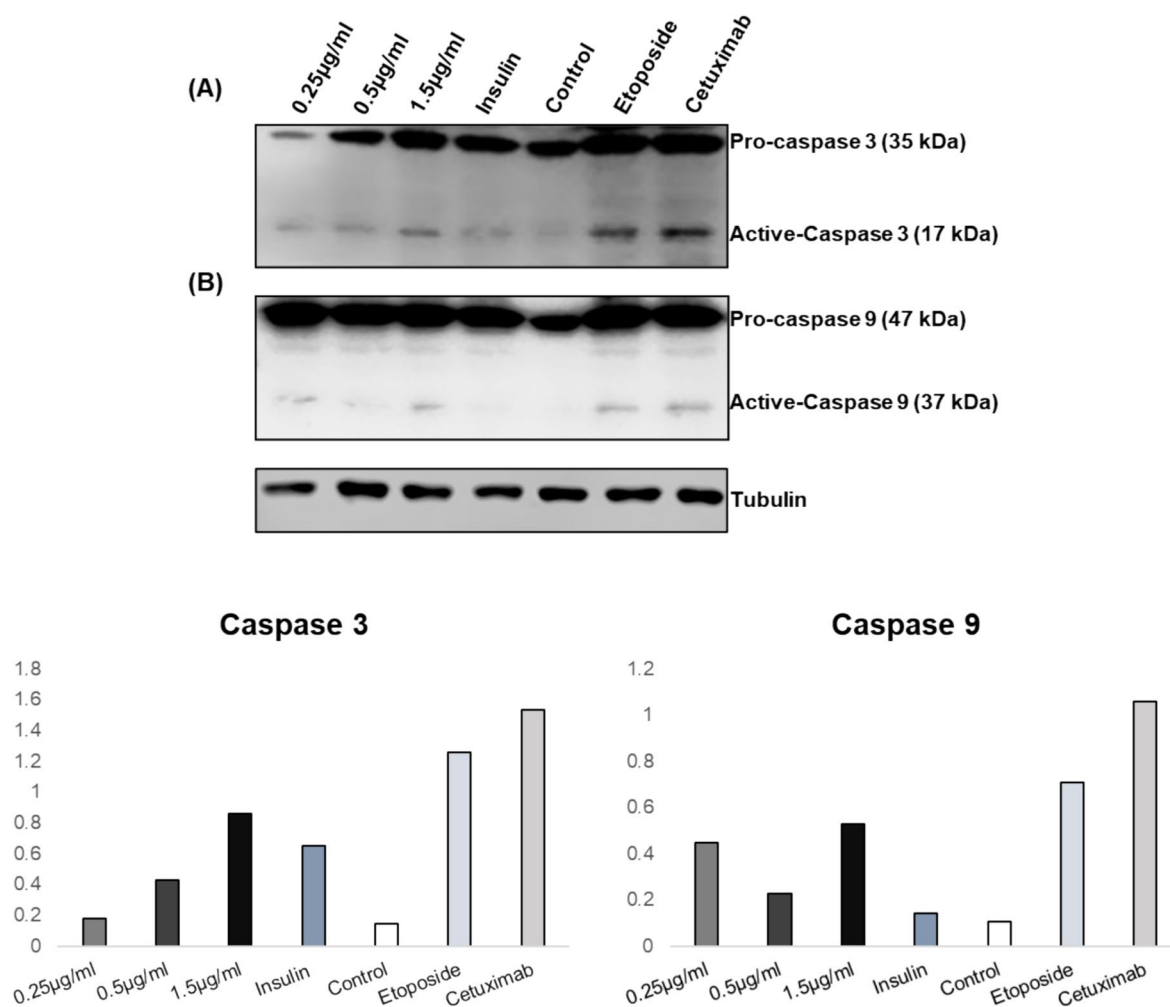


**Fig. 6** Caspase activity of TrkB-IgL 5.11 mAb in HCT116 cells in a dose-dependent manner. HCT116 cells were treated for 12 h with varying concentrations of TrkB-IgL 5.11 mAb, with Etoposide and

Cetuximab as positive controls, and Insulin as a negative control. Untreated cells were used as a baseline control

activation and consequently inhibiting signal transduction of the RAS/RAF/MEK/ERK and PI3K/AKT pathways. This leads to cell cycle arrest and/or induction of apoptosis (Son et al. 2015; Okada et al. 2014; Marzi et al. 2016).

At a concentration of 10 µg/ml, TrkB-IgL 5.11, 4.11, and 4.6 did not affect cell viability, while TrkB-IgL 4.3 and 5 µg/ml Etoposide exhibited toxic effects on both cancer cell lines (Fig. 4C, D).

The effect of the purified mAbs on cell proliferation was evaluated similarly. The xCELLigence results revealed that the whole purified antibody demonstrated suppression of cell proliferation compared to both positive and negative controls in targeting cancer cells (Fig. 4E, F).

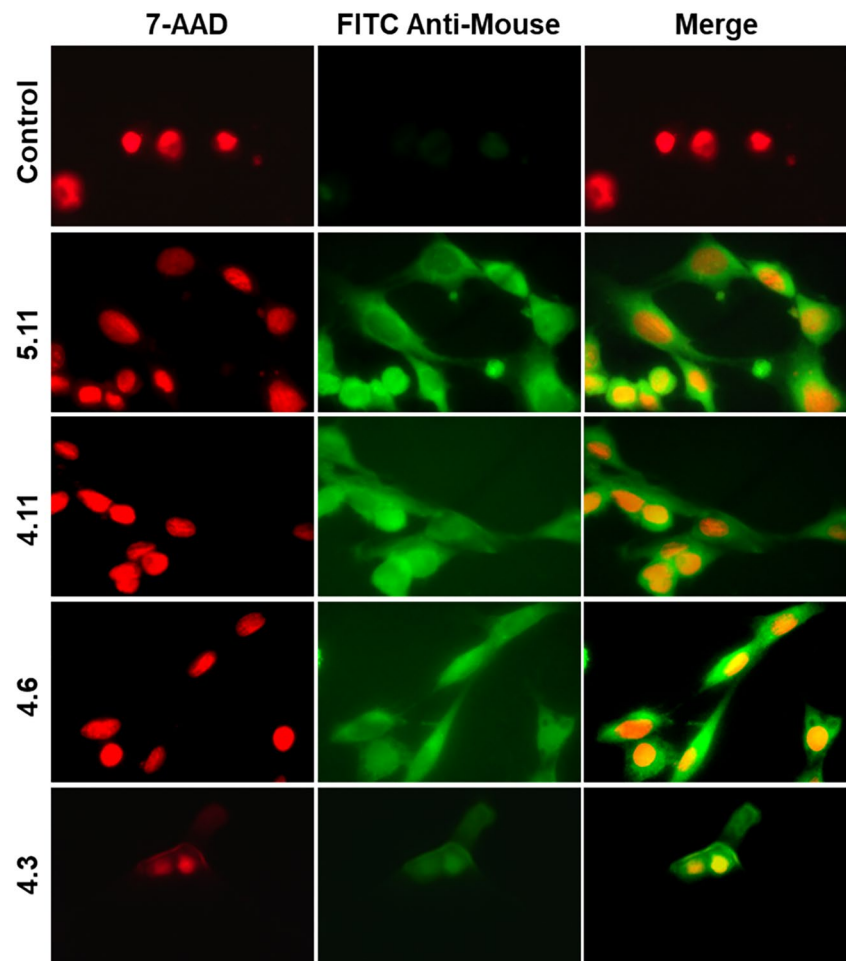
While other purified antibodies did not show an effective response, Western blot analysis confirmed that the TrkB-IgL 5.11 mAb effectively suppressed the phosphorylation of TrkB and its downstream effectors, AKT and ERK, indicating a blockade of the signaling pathways essential for cancer

cell survival (Fig. 5). Additionally, the 5.11 mAb induced apoptosis in HCT116 cells, as evidenced by increased activities of Caspase-3 and Caspase-9, highlighting its potential as a therapeutic agent (Fig. 6). This apoptotic induction underscores the therapeutic potential of TrkB-IgL 5.11 mAb in targeting cancer cells not only by inhibiting growth but also by promoting programmed cell death.

Immunofluorescence labeling experiments showed that all purified antibodies localized to the membrane of SHSY5Y cells (Fig. 7). This indicated that the antibodies specifically bound to membrane targets and effectively interacted with them, suggesting their potential for targeting membrane-associated antigens in therapeutic applications.

All the data obtained show that the TrkB-IgL 5.11 antibody, produced by targeting the TrkB receptor, has an effective neutralizing effect on human breast cancer and human colon cancer cells compared to other purified TrkB-IgL antibodies. These findings suggest that the epitope recognized

**Fig. 7** Immunofluorescence staining showing TrkB receptor distribution and localization in SH-SY5Y cells. The cells were grown on coverslips and treated with anti-TrkB IgL mAbs followed by an anti-mouse FITC secondary antibody (green) to detect their localization on the membrane. Nuclei were stained with 7-AAD (red). 7-AAD and FITC images were merged



by the antibody might be a critical domain regulating TrkB inactivation, as it appears to contain a region capable of neutralizing the receptor. It should also be noted that 5.11 was isolated in its full purity.

Based on these results, a new hypothesis was proposed: the Ig-like type 1 and Ig-like type 2 domains could be produced as separate recombinant peptides and then subjected to neutralization tests to evaluate the specificity of the epitope. Additionally, the low molecular weight mature form of BDNF, which binds to TrkB, could be produced recombinantly, allowing for competitive inhibition tests using existing anti-TrkB antibodies.

**Supplementary Information** The online version contains supplementary material available at <https://doi.org/10.1007/s13205-024-04063-x>.

**Author contributions** GEY designed and performed the experiments and analyzed the data, performed the image analysis, prepared the figures and wrote the manuscript. EY planned, supervised, and analysis of the results and revised the manuscript.

**Funding** Supported by TÜBİTAK.

**Data and materials availability** All presented data and materials are included in this article.

## Declarations

**Conflict of interest** The authors declare no conflicts of interest.

## References

- Arevalo JC, Wu SH (2006) Neurotrophin signaling: many exciting surprises! *Cell Mol Life Sci* 63:1523–1537
- Day TW, Ching-Huang Wu, Safa AR (2009) Etoposide induces protein kinase C $\delta$ - and caspase-3-dependent apoptosis in neuroblastoma cancer cells. *Mol Pharmacol* 76:632–640
- de Farias B, Caroline DB, Rosemberg TE, Heinen P-S, Abujamra AL, Kapczinski F, Brunetto AL, Ashton-Prolla P, Meurer L, Bogo MR (2011) BDNF/TrkB content and interaction with gastrin-releasing peptide receptor blockade in colorectal cancer. *Oncology* 79:430–439
- Desmet CJ, Peeper DS (2006) The neurotrophic receptor TrkB: a drug target in anti-cancer therapy? *Cell Mol Life Sci* 63:755–759
- Goloudina AR, Demidov ON, Garrido C (2012) Inhibition of HSP70: a challenging anti-cancer strategy. *Cancer Lett* 325:117–124
- Guo D, Hou X, Zhang H, Sun W, Zhu L, Liang J, Jiang X (2011) More expressions of BDNF and TrkB in multiple hepatocellular

- carcinoma and anti-BDNF or K252a induced apoptosis, suppressed invasion of HepG2 and HCCLM3 cells. *J Exp Clin Cancer Res* 30:1–8
- Guzel TA, Mech K, Wroński M, Gerkowicz K, Bednarczyk A, Adamczyk W, Radecka M, Słodkowski M (2021) Brain-derived neurotrophic factor in gastroenterology oncology—short review of current literature. *Ann Agric Environ Med* 28:367–371
- Haniu M, Montestruque S, Bures EJ, Talvenheimo J, Toso R, Lewis-Sandy S, Welcher AA, Rohde MF (1997) Interactions between brain-derived neurotrophic factor and the TRKB receptor. *J Biol Chem* 272:25296–25303
- Hellweg R, Schulte-Herbruggen O, Jockers-Scherubl MC (2008) Neurotrophins—from pathophysiology to treatment in Alzheimer's disease. *Curr Alzheimer Res* 5:38–44
- Huang EJ, Reichardt LF (2003) Trk receptors: roles in neuronal signal transduction. *Annu Rev Biochem* 72:609–642
- Jin Z, Yifan Lu, Xiongyan Wu, Pan T, Zhenjia Yu, Hou J, Airong Wu, Li J, Yang Z, Li C (2021) The cross-talk between tumor cells and activated fibroblasts mediated by lactate/BDNF/TrkB signaling promotes acquired resistance to anlotinib in human gastric cancer. *Redox Biol* 46:102076
- Kelly-Spratt KS, Klesse LJ, Parada LF (2002) BDNF activated TrkB/IRR receptor chimera promotes survival of sympathetic neurons through Ras and PI-3 kinase signaling. *J Neurosci Res* 69:151–159
- Klein R, Parada LF, Coulier F, Barbacid M (1989) trkB, a novel tyrosine protein kinase receptor expressed during mouse neural development. *EMBO J* 8:3701–3709
- Klein R, Smeyne RJ, Wurst W, Long LK, Anna Auerbach B, Joyner AL, Barbacid M (1993) Targeted disruption of the trkB neurotrophin receptor gene results in nervous system lesions and neonatal death. *Cell* 75:113–122
- Lam C-T, Yang Z-F, Lau C-K, Tam K-H, Fan S-T, Poon RTP (2011) Brain-derived neurotrophic factor promotes tumorigenesis via induction of neovascularization: implication in hepatocellular carcinoma. *Clin Cancer Res* 17:3123–3133
- Lopez-Suarez L, Al Awabdh S, Coumoul X, Chauvet C (2022) The SH-SY5Y human neuroblastoma cell line, a relevant in vitro cell model for investigating neurotoxicology in human: focus on organic pollutants. *Neurotoxicology*. 92:131–155. <https://doi.org/10.1016/j.neuro.2022.07.008>
- Marzi L, Combes E, Vié N, Ayrolles-Torro A, Tosi D, Desigaud D, Perez-Gracia E, Larbouret C, Montagut C, Iglesias M (2016) FOXO3a and the MAPK p38 are activated by cetuximab to induce cell death and inhibit cell proliferation and their expression predicts cetuximab efficacy in colorectal cancer. *Br J Cancer* 115:1223–1233
- Meng L, Liu B, Ji R, Jiang X, Yan X, Xin Y (2019) Targeting the BDNF/TrkB pathway for the treatment of tumors. *Oncol Lett* 17:2031–2039
- Middlemas DS, Lindberg RA, Hunter T (1991) trkB, a neural receptor protein-tyrosine kinase: evidence for a full-length and two truncated receptors. *Mol Cell Biol* 11:143–153
- Nakagawara A (2001) Trk receptor tyrosine kinases: a bridge between cancer and neural development. *Cancer Lett* 169:107–114
- Numakawa T, Adachi N, Richards M, Chiba S, Kunugi H (2013) Brain-derived neurotrophic factor and glucocorticoids: reciprocal influence on the central nervous system. *Neuroscience* 239:157–172
- Okada Y, Miyamoto H, Goji T, Takayama T (2014) Biomarkers for predicting the efficacy of anti-epidermal growth factor receptor antibody in the treatment of colorectal cancer. *Digestion* 89:18–23
- Okamura K, Harada T, Wang S, Ijichi K, Furuyama K, Koga T, Okamoto T, Takayama K, Yano T, Nakanishi Y (2012) Expression of TrkB and BDNF is associated with poor prognosis in non-small cell lung cancer. *Lung Cancer* 78:100–106
- Okugawa Y, Tanaka K, Inoue Y, Kawamura M, Kawamoto A, Hiro J, Saigusa S, Toiyama Y, Ohi M, Uchida K (2013) Brain-derived neurotrophic factor/tropomyosin-related kinase B pathway in gastric cancer. *Br J Cancer* 108:121–130
- Qian MD, Zhang J, Tan X-Y, Wood A, Gill D, Cho S (2006) Novel agonist monoclonal antibodies activate TrkB receptors and demonstrate potent neurotrophic activities. *J Neurosci* 26:9394–9403
- Shoval G, Weizman A (2005) The possible role of neurotrophins in the pathogenesis and therapy of schizophrenia. *Eur Neuropsychopharmacol* 15:319–329
- Son DJ, Hong JE, Ban JO, Park JH, Lee HL, Gu SM, Hwang JY, Jung MH, Lee DW, Han SB, Hong JT (2015) Synergistic inhibitory effects of cetuximab and cisplatin on human colon cancer cell growth via inhibition of the ERK-dependent EGF receptor signaling pathway. *BioMed Res Int*. <https://doi.org/10.1155/2015/397563>
- Tajbakhsh A, Mokhtari-Zaer A, Rezaee M, Afzaljavan F, Rivandi M, Hassanian SM, Ferns GA, Pasdar A, Avan A (2017) Therapeutic potentials of BDNF/TrkB in breast cancer; current status and perspectives. *J Cell Biochem* 118:2502–2515
- Tanaka K, Okugawa Y, Toiyama Y, Inoue Y, Saigusa S, Kawamura M, Araki T, Uchida K, Mohri Y, Kusunoki M (2014) Brain-derived neurotrophic factor (BDNF)-induced tropomyosin-related kinase B (Trk B) signaling is a potential therapeutic target for peritoneal carcinomatosis arising from colorectal cancer. *PLoS One* 9:e96410
- Thiele CJ, Li Z, McKee AE (2009) On Trk—the TrkB signal transduction pathway is an increasingly important target in cancer biology. *Clin Cancer Res* 15:5962–5967
- Wu C-H, Chen C-C, Hung T-H, Chuang Y-C, Chao M, Shyue S-K, Chen S-F (2019) Activation of TrkB/Akt signaling by a TrkB receptor agonist improves long-term histological and functional outcomes in experimental intracerebral hemorrhage. *J Biomed Sci* 26:1–16
- Xu Y, Jiang W-G, Wang H-C, Martin T, Zeng Y-X, Zhang J, Qi Y-S (2019) BDNF activates TrkB/PLCγ1 signaling pathway to promote proliferation and invasion of ovarian cancer cells through inhibition of apoptosis. *Eur Rev Med Pharmacol Sci* 23:5093–5100
- Yoshii A, Constantine-Paton M (2010) Postsynaptic BDNF-TrkB signaling in synapse maturation, plasticity, and disease. *Dev Neurobiol* 70:304–322
- Zaccaro MC, Ivanisevic L, Perez P, Meakin SO, Uri Saragovi H (2001) p75 Co-receptors regulate ligand-dependent and ligand-independent Trk receptor activation, in part by altering Trk docking subdomains. *J Biol Chem* 276:31023–31029

Springer Nature or its licensor (e.g. a society or other partner) holds exclusive rights to this article under a publishing agreement with the author(s) or other rightsholder(s); author self-archiving of the accepted manuscript version of this article is solely governed by the terms of such publishing agreement and applicable law.